FINAL TECHNICAL REPORT

EARTHQUAKE POTENTIAL IN THE SAN FRANCISCO AREA FROM PS-INSAR MEASUREMENTS

National Earthquake Hazard Reduction Program

U.S. Geological Survey

NEHRP Program Element: I, Products for Earthquake Loss Reduction

Award Number: 07-HQGR-0077

Principal investigator:

Roland Bürgmann

University of California, Berkeley
Department of Earth and Planetary Science
307 McCone Hall
Berkeley, CA 94720-4767
Telephone: (510) 643-9545;
Fax:(510) 643-9980;
e-mail: burgmann@seismo.berkeley.edu

EARTHQUAKE POTENTIAL IN THE SAN FRANCISCO AREA FROM PS-INSAR MEASUREMENTS

Award Number: 07-HQGR-0077

Roland Bürgmann

University of California, Berkeley
Department of Earth and Planetary Science
307 McCone Hall
Berkeley, CA 94720-4767
Telephone: (510) 643-9545;
Fax:(510) 643-9980;
E-mail: burgmann@seismo.berkeley.edu

Technical abstract:

Our investigations aim to constrain active tectonic and non-tectonic deformation, fault slip rates and the distribution of aseismic slip relying on permanent scatterer radar interferometry (PS-InSAR) satellite measurements. The space geodetic measurements provide information on the nature of elastic strain accumulation about seismogenic faults, their locking depth and slip rates, and any variations of those parameters in space and time. We utilize the surface deformation measurements and elastic dislocation mdeols to determine the distribution of locked and creeping sections along the Calaveras-Hayward-Rodgers Creek fault zone. Inversions of these data reveal a locked zone at depth which has built up a slip deficit since the 1868 Hayward fault rupture that is large enough to produce a M > 6.7 earthquake. Our inversions and the distribution of repeating microearthquakes show that a shallow aseismically creeping fault surface directly connects the central Calaveras and southern Hayward fault at depth. The Rodgers Creek fault is also recognized to creep at 4-6 mm/yr in the upper ~5km of the crust near Santa Rosa. Increasingly detailed models of the fault slip process illuminate the locked source areas of past and future large earthquakes along these faults.

Non-technical abstract:

Measurements of surface deformation from range change rates determined with satellite radar interferometry (InSAR) allow us to image tectonic surface motions in the San Francisco Bay Area at great precision. We utilize these measurements to determine the distribution of locked and creeping sections along the Calaveras-Hayward-Rodgers Creek fault zone. These data reveal a locked zone at depth along the Hayward fault which has built up a slip deficit since the 1868 earthquake that is large enough to produce a $M > 6.7$ earthquake. We find that a shallow aseismically creeping fault surface connects the central Calaveras and southern Hayward fault at depth. Near Santa Rosa, the Rodgers Creek fault is also recognized to creep in the shallow part of the crust suggesting a slightly reduced earthquake potential along this section of the fault. Increasingly detailed models of the fault slip process illuminate the locked source areas of past and future large earthquakes along these faults which help inform earthquake hazard estimates and simulations of future earthquake shaking.

EARTHQUAKE POTENTIAL IN THE SAN FRANCISCO AREA FROM PS-INSAR MEASUREMENTS

1. INTRODUCTION

1.1 Project components

Our investigations aim to constrain secular fault slip rates and the distribution of aseismic slip. Geodetic measurements provide information on the nature of elastic strain accumulation about seismogenic faults, their locking depth and slip rates, and any variations of those parameters in space and time. This research relies on the analysis and modeling of space geodetic data and interpretation of those results in the context of their mechanical behavior and earthquake potential. GPS and InSAR are complementary techniques for making precise measurements of displacements of the Earth's surface. These can be related to sources of deformation at depth (e.g. faults) by mechanical models. We formally invert the geodetic data for model fault parameters such as depth of locking and slip rate.

This project aimed to further develop PS-InSAR analysis towards the study of active deformation in the San Francisco Bay region and improve the spatial and temporal resolution of surface deformation. By expanding the analysis to span more time and including data from multiple SAR-viewing geometries and spacecraft, we continue to make significant and essential advances that address specific goals of the NEHRP program aimed at reducing earthquake losses.

2. OBSERVATIONS

2.1 GPS data

The utility of the PS-InSAR data for crustal deformation and earthquake potential studies is greatly enhanced by the availability of the high-precision GPS velocity field reduces some long-wavelength error sources, puts the interferogrametric data into a consistent reference frame, and helps resolve vertical from horizontal velocity contributions to the range-change signal (Bürgmann et al., 2006). A mix of campaign mode (SGPS) yearly GPS measurements and data from a core network of continuously operating GPS stations (CGPS) of the BARD and PBO networks contribute to a precise (at mm/yr level) representation of the surface velocity field.

Over the last decade, we have developed the BAVU (Bay Area Velocity Unification) compilation of continuous GPS data from the BARD network and campaign data (d'Alessio et al., 2005). The BAVU compilation includes survey-mode GPS data from over 200 GPS stations throughout the greater San Francisco Bay Area from Sacramento to San Luis Obispo collected from 1991 to 2007 by U. C. Berkeley, the U.S. Geological Survey, the California Department of Transportation, Stanford University, U. C. Davis and the Geophysical Institute in Fairbanks, AK. The sparsely distributed, but continuously operating CGPS BARD and PBO networks provide a precise 3D geodetic framework with high temporal resolution. Repeated campaign GPS measurements in the Bay Area by our group and data obtained by the USGS provide appropriate densification of precise regional surface velocities to determine long-term deformation rates. See http://seismo.berkeley.edu/~burgmann/RESEARCH/BAVU/index.html for data products and further information. Figure 1 shows the most recent update of the GPS velocity field.

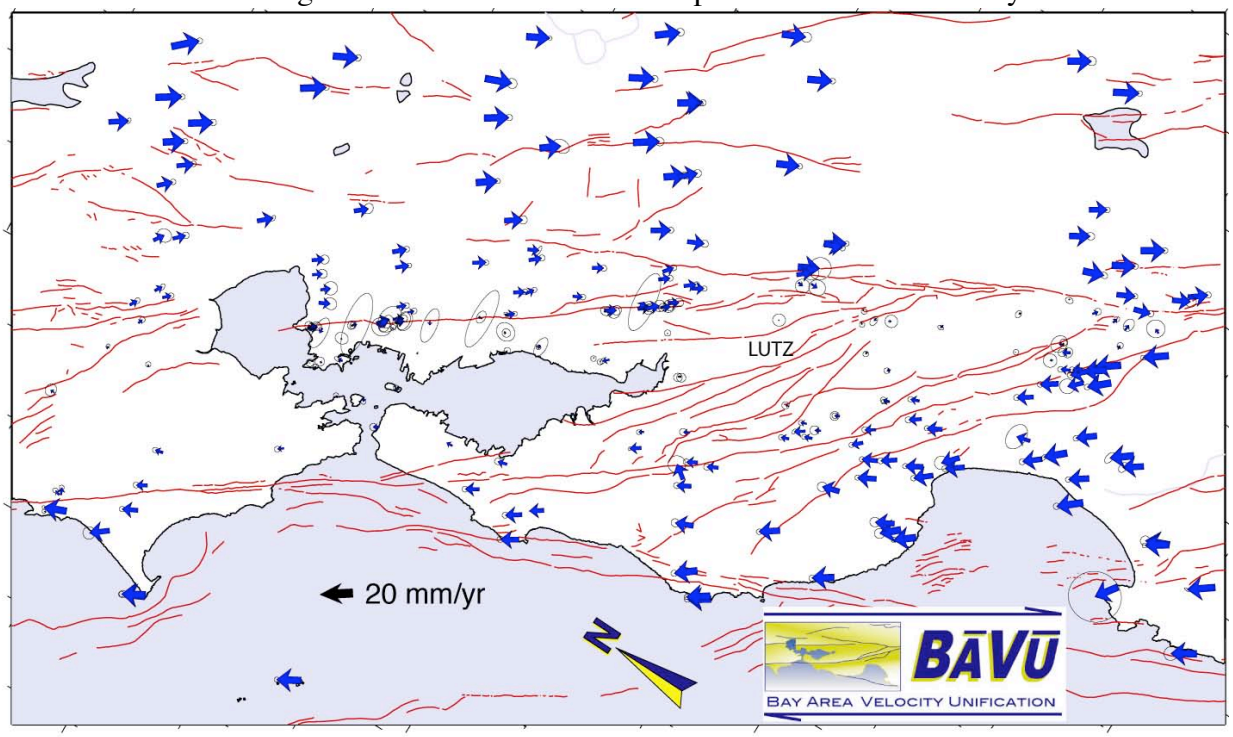

Figure 1. Updated BAVU velocity field referenced to a local site (LUTZ) on the central Bay Block spanning 1994-2006. The map is in an oblique Mercator projection about the pole of Pacific-plate-to-SNGV block rotation.

2.2 PS-InSAR data

InSAR provides a one-dimensional measurement of change in distance along the look direction of the radar spacecraft. Given the orientation of the track direction of polar, sun-synchronous satellites, this measurement is affected by deformation in both horizontal components and, particularly, in the vertical. We have had significant success in the recent past in applying conventional InSAR to both the horizontal and the vertical surface deformation in the San Francisco Bay Area, revealing cm-level uplift and subsidence patterns related to the seasonal drawdown and recharge of the Santa Clara valley aquifer (Schmidt and Bürgmann, 2003); rapid motions of deep-seated landslides (Hilley et al., 2004); a possible sub-mm/yr contribution of an east-side-up, dip-slip component to the range change offset across the creeping northern Hayward fault (Hilley et al., 2004; Schmidt et al., 2005); and allowing the estimation of the distribution of fault creep on the Hayward fault, and therefore the extent of the part of that fault that remains locked (Schmidt et al., 2005). Recent work during the project period using the PS-InSAR data in conjunction with our GPS measurements has focused on resolving vertical motion in the Bay region (Bürgmann et al., 2006) and on resolving aseismic slip on the Hayward-Rodgers Creek faults (Funning et al., 2007).

Permanent or persistent scatterer InSAR (PS-InSAR) is a recent development in InSAR processing. Using the radar returns from phase-stable targets on the ground, it is possible to generate a time series of surface displacement changes, with atmospheric effects mitigated (Ferretti et al., 2004; Ferretti et al., 2001). Such stable targets, referred to as persistent scatterers, or 'PS', can be identified independently of the stability of their neighbors, a capability that has already been demonstrated to dramatically increase the spatial coverage of observations in areas where there are buildings (which are phase stable) surrounded by vegetation (which is not) when compared to conventional interferometry.

This approach allows many more SAR images to be used, allowing the estimation and removal of the effects of atmospheric perturbations from the data. This is achieved by spatiotemporal filtering. Geophysical signals, such as fault creep are considered to be correlated in time; atmospheric signals are assumed to *only* be correlated in space. Following subtraction of the estimated atmospheric effects, a best-fitting linear velocity is then computed for the displacement time series of each PS. The end product is a map of surface deformation velocities, projected into the line-of-sight (LOS) of the observing satellite (Figure 2).

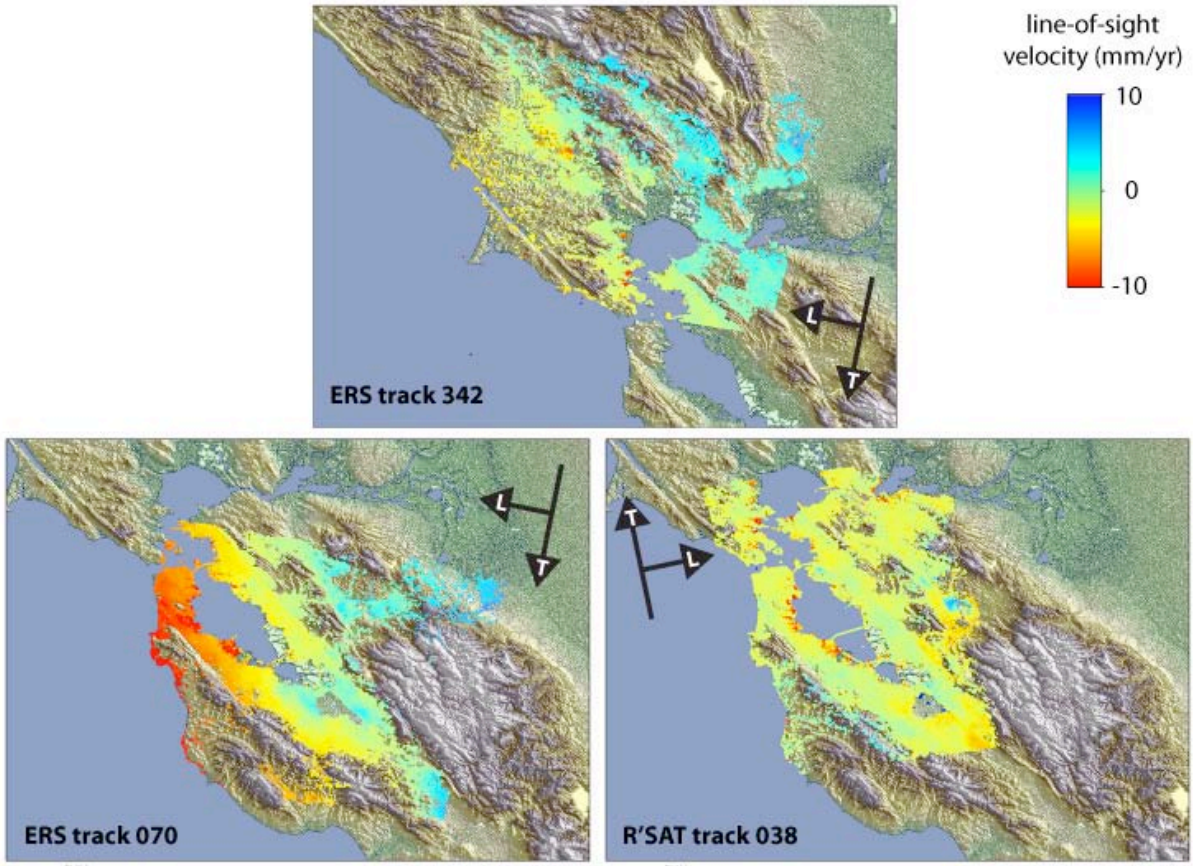

Figure 1: PS-InSAR data for the San Francisco Bay Area. Sudden steps in color across linear features are indicators of fault creep. For scale, the width of the zone covered by a single ERS track is approximately 100 km.

Currently, three PS-INSAR datasets exist for the San Francisco Bay Area (Figure 2; Table 1), each covering part of the northern Calaveras, Hayward or Rodgers Creek faults. Two of the datasets are descending track datasets (westward-looking) acquired by the European Space Agency (ESA) ERS satellites, the other is an ascending track dataset (eastward-looking), acquired by the Canadian Space Agency RADARSAT platform. The combination of ascending and descending data coverage potentially allows discrimination between horizontal and vertical motions, and can thus assist attribution of causes to observed deformation signals. The numbers of persistent scatterers (PS) range between 71,000 for the northernmost scene (ERS track 342), which has the lowest density of development, and was composed from the fewest datapoints, up to 225,000 for the RADARSAT ascending dataset, the variability reflecting differences in instrument polarization, data volume and satellite orbital repeat time. oints whose displacements vary in a highly non-linear fashion, such as a large area of rapid seasonal uplift and subsidence in the Santa Clara Valley (Schmidt and Bürgmann, 2003) are excluded from the final data set. In

addition, this dataset contains time-series of displacement, which allow us to identify regions in which there is a significant time-varying, often seasonal component to the deformation field.

Dataset	No. of images	Time interval	Asc./desc.	No. of PS
ERS track 70	49	1992-2000	Desc.	115,000
ERS track 342	30	1992-2001	Desc.	71,000
RADARSAT track 38	46	1998-2006	Desc.	225,000

Table 1: Details of existing PS-InSAR datasets covering the target fault zone.

When interpreted in terms of vertical motions, the residual range-change rate field of bedrock target points includes three larger areas of subsidence and three regions of uplift at 0.5-1.5 mm/yr rate (Figure 3). One area of apparent subsidence is located east of the Greenville fault and we have no obvious explanation for this feature. The second area of subsidence at rates of up to ~2 mm/yr appears localized about the epicentral region of the 1989, $M_w = 6.9$ Loma Prieta earthquake and coincides with the region of horizontal contraction evident in the residual GPS velocities. A third zone of slow (~0.5 mm/yr) subsidence along the northern San Francisco peninsula may be related to an extensional bend in the SAF and/or interaction with the offshore San Gregorio fault zone. Uplifted regions along the East Bay Hills, the Santa Cruz Mountains to the northeast of the SAF near Black Mountain and in the southern foothills of Mt. Diablo appear to reflect tectonic uplift along restraining discontinuities of Bay Area strike-slip faults (Bürgmann et al., 2006).

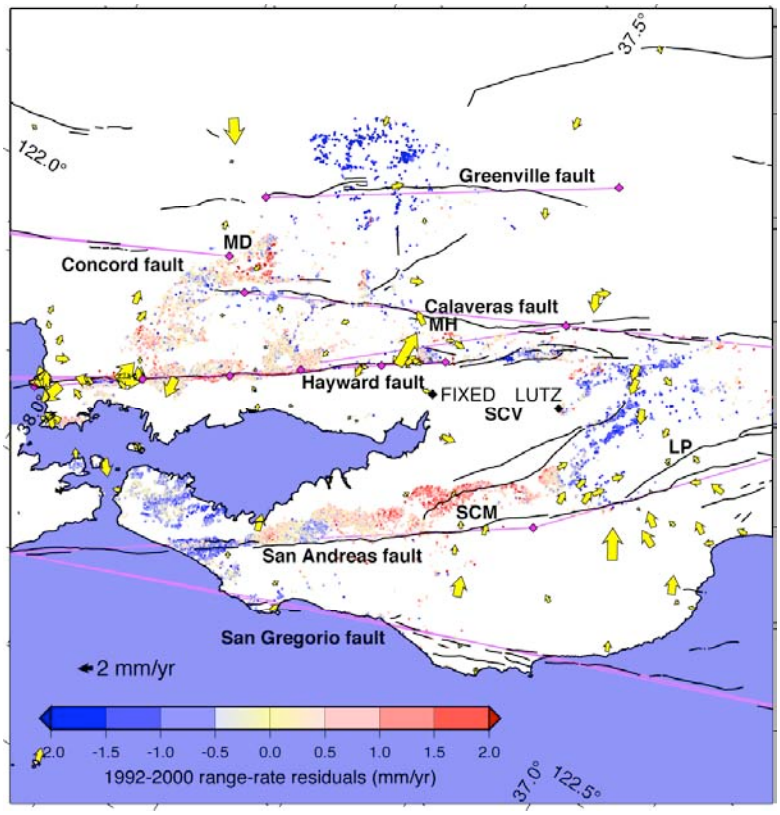

Figure 3: Residual surface velocities after correction for the horizontal strain field due to strike-slip faulting. Only PS points located on bedrock are shown, to ensure that non-tectonic signals related to the behavior of Quaternary substrate are removed. Areas of red here indicate uplifiting zones; conversely, blue areas indicate subsidence. Yellow arrows are the residuals of the fit of the dislocation model to the GPS data. Note the uplift signals associated with Mount Diablo (MD), the Santa Cruz Mountains (SCM) and the Mission Hills (MH), and the subsidence seen at Loma Prieta (LP). Purple lines are the surface projections of the shallow and/or deep dislocations used to model the horizontal strain field.

Recently, we signficantly expanded the coverage of the PS-InSAR analysis along track 70, providing a comprehensive image of surface deformation along a 200-km-long swath (Figure 4). These data will provide the basis of research on the follow-up project of this work which is focused on the Sacramento Delta and eastern Coast Ranges foothills area. We are excited about the potential of this data set for study of active tectonic deformation and uplift in the eastern Bay area, land subsidence and levee deformation in the Delta region and aseismic slip along the Concord – Green Valley fault zone.

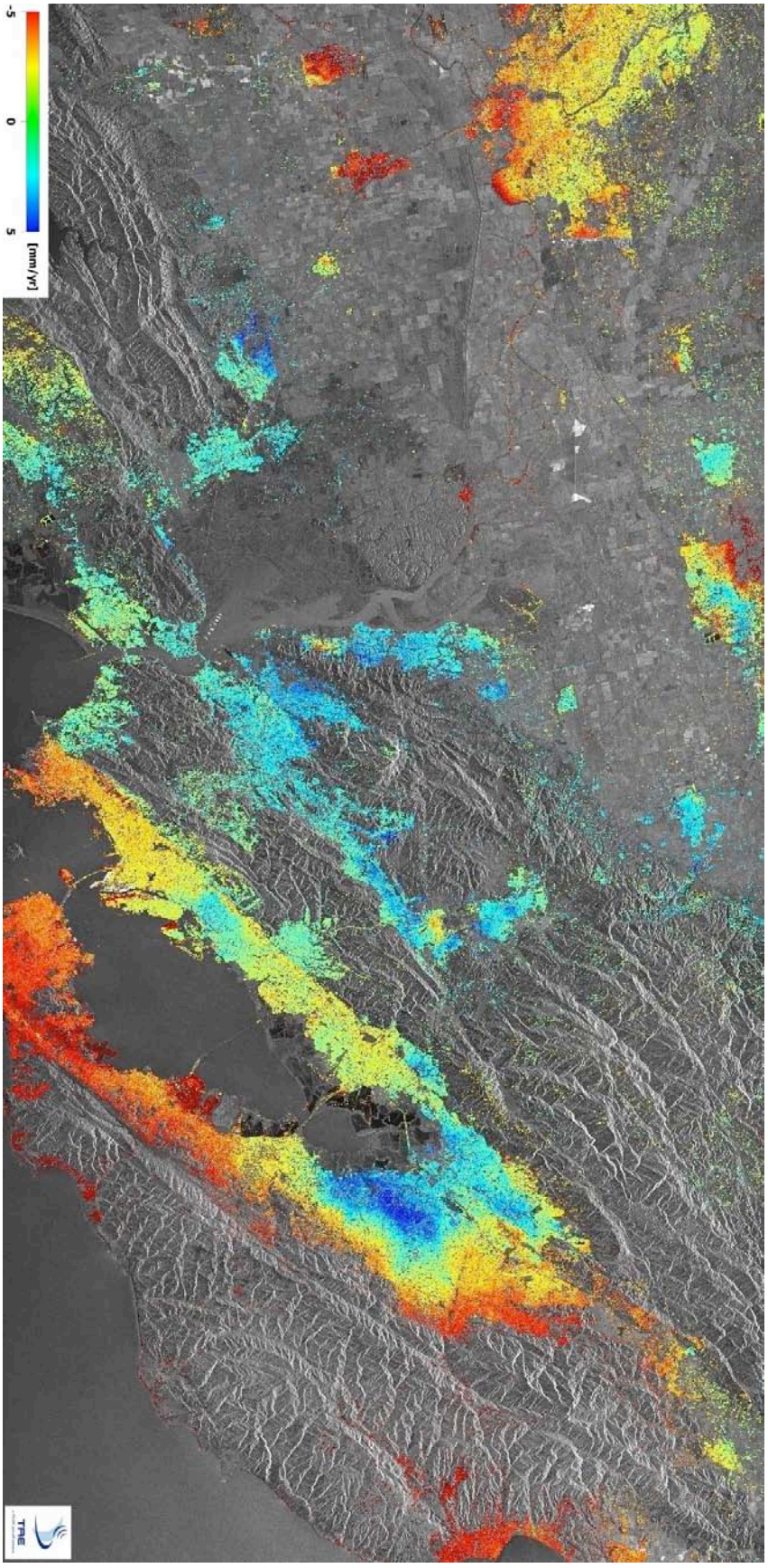

Figure 4: Recently completed PS-InSAR range change velocity map over Bay area, eastern Coast Ranges, Sacramento Delta and Great Valley. Red colors indicated subsidence or westward motion, blue colors suggest uplift or eastward motions. The Sacramento urban area is at the top right of the image. We note rapid subsidence across the delta region, creep along the Concord – Green Valley fault, and an intriguing uplift signal near Vacaville.

3. RESULTS

3.1 Hayward Fault Earthquake Potential

A significant portion of our research continues to focus on the earthquake potential of the Hayward fault. This is work carried out with postdoctoral fellow Gareth Funning, who recently accepted a faculty position at the University California, Riverside. A manuscript, to be submitted to Science is currently in preparation. The Hayward fault accommodates strain in two different ways - in large (M~7) earthquakes, and by aseismic creep. In combination with its northern extension, the Rodgers Creek fault, it is currently considered the most dangerous fault in northern California. The presence of creep is significant in terms of the seismic hazard posed by the fault - areas that undergo creep dissipate strain that may otherwise be released seismically. It is also significant in terms of its effect on the surface, causing detectable deformation. Results from this project demonstrate that a spatially dense dataset of surface deformation rates, generated from advanced processing of satellite radar images, enables us to map out which areas of the fault are creeping - and also, therefore, which areas are locked and accumulating strain for the next major earthquake.

Creep on the Hayward fault was first identified by Cluff & Steinbrugge (1966), and has been monitored for over 30 years in some locations using alignment arrays (Galehouse and Lienkaemper, 2003; Lienkaemper et al., 2001). Variations in creep rate are observed along the length of the fault; Simpson et al. (2001) noted, using simple boundary element dislocation models, that such variations are consistent with variations in depth of creep. Similar behavior was noted by Malservisi et al. (2003) in finite element models. However, surface creep data alone provide only weak constraints on the distribution of creep with depth. Latterly, InSAR data, in conjunction with GPS and microearthquake data, have been used to estimate the creep distribution on the upper 12 km of the fault using dislocation models (Bürgmann et al., 2000; Schmidt et al., 2005), with an attendant improvement in depth resolution. However, temporal decorrelation of data, especially on the vegetated northeastern side of the fault, restricts the data coverage at distances > 5 km from the fault, and therefore the resolution on the fault at depth could still be improved.

PS-InSAR data are one means through which we can improve our resolution yet further, through increased density of datapoints east of the fault. All three existing PS-InSAR datasets cover the Hayward fault in part, and so were used here. In order to strip out the redundancy in our data prior to modeling, we subsampled them by considering where data would be necessary to resolve creep on the fault, (Funning et al., 2007). In addition, we incorporated over 130 GPS velocities from the BAVU compilation (d'Alessio et al., 2005), in order to better constrain the

regional strain field, and published alignment array data (Lienkaemper et al., 2001) to accurately constrain the near-field fault offset rate. The results shown here are currently being written up for publication (G J Funning et al., manuscript in preparation, 2008).

3.1.1. Kinematic modeling

We rely on both descending (westward looking, ERS track 70 data) and ascending (eastward looking RADARSAT-1 data) to determine the deformation field near and aseismic slip along the Hayward fault (Figure 5). The data are modeled in two stages. First, we produce a kinematic model of the deformation. Assuming the deformation can be modeled as occurring within an elastic half space, we define a Hayward fault geometry assembled from a mesh of triangular dislocations, based upon microearthquake locations (after Schmidt et al., 2005), with additional deep dislocations located beneath all of the major Bay Area faults (e.g. the San Andreas, Calaveras and San Gregorio faults as well as the Hayward fault), in order to model the regional strain field. Data kernels relating slip on each dislocation to each datapoint are calculated using the Poly3D software (Thomas and Pollard, 1993), and inverted using a non-negative least squares algorithm and with appropriate smoothing. Relative weighting of PS-InSAR and GPS data are achieved by using modelled and formal covariances, respectively. The resultant model (Figure 5) shows creep occurring at rates between 3 and 8 mm/yr over the majority of the fault plane. The highest creep rates occur in the vicinity of Fremont, and are consistent with surface measurements from that location, which were not incorporated in this inversion.

A low creep zone (< 1 mm/yr) exists along the central part of the fault, an approximately 40 km long zone between Oakland and ending just north of Fremont, from the base of the upper crust (12 km) up to around 4 km depth in the north, down to an average of ~6 km depth at its southern end. The northernmost portion of the fault also shows low creep north of Pt Pinole, where the Hayward fault goes offshore into San Pablo Bay, however this is most likely a consequence of a lack of data coverage in those areas. The low creep zone is likely to represent an area which is effectively locked and accumulating significant elastic strain, and which may thus rupture in a future earthquake.

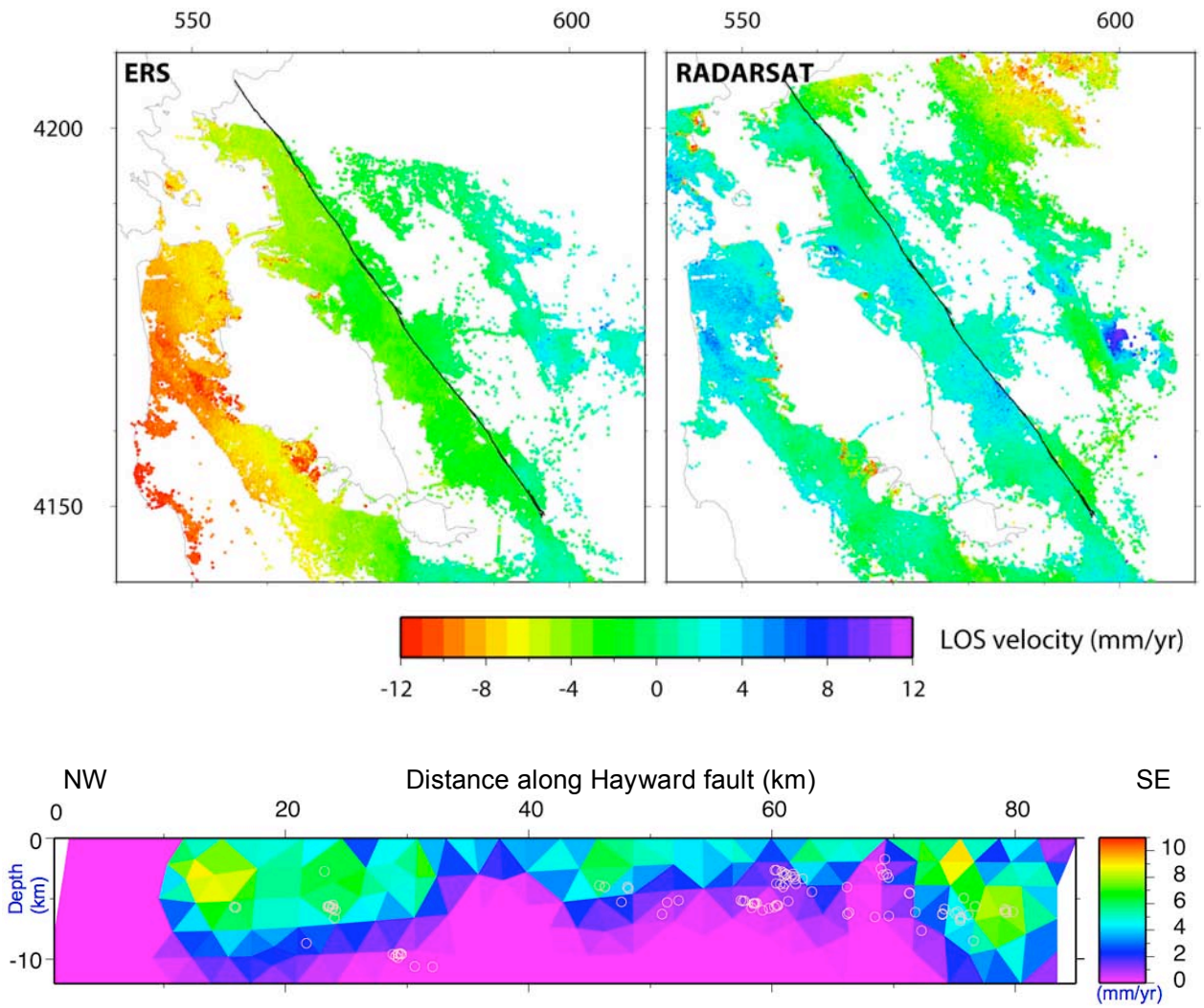

Figure 5. Top: PS velocities for the San Francisco Bay Area, in the satellite line-of-sight (LOS) direction for 1992-2000 ERS-descending-orbit (49 acquisitions) and 2001-2006 RADARSAT ascending-orbit (35 acquisitions) data. The Hayward fault is marked as a solid black line. Note that there is significant coverage to the east of the fault, an area unsuitable for conventional InSAR due to heavy vegetation. **Bottom:** Model of average sub-surface fault creep rates (in mm/yr) on upper 12 km of the Hayward fault. The model is based on inversion of the InSAR LOS velocities and GPS data in the region. The magenta (fully locked) region represents the likely source region of 1868-type M=7 earthquakes, which repeat on average every 140 years.

3.1.2. Boundary element modeling

In order to obtain a mechanically consistent model of creep on the Hayward fault, and to estimate the dimensions of the area which is fully locked, we calculate a suite of boundary element models (BEMs), again using the same triangular fault mesh for the Hayward fault and the Poly3D software. We assume that the system is driven from below by slip on the same deep dislocations that were used in the kinematic modeling, and at the same rates as obtained from

that inversion. To represent creeping or locking on the fault plane, we specify boundary conditions of zero shear traction or zero displacement, respectively, for individual triangular elements of the fault mesh. Thus the 'creeping' portions of the fault are able to slip frictionlessly and instantaneously if loaded by stresses from the driving faults.

If the system were driven with no locked patches (e.g. Figure 6b), a maximum creep rate of ~10.5 mm/yr is obtained in the central portion of the fault. This maximum is slightly higher than the driving slip rate beneath the fault (~9.5 mm/yr), due to additional loading from the Hayward fault's neighbors (i.e. the Calaveras and San Andreas faults). Creep rates drop off towards the ends of the fault. This is due to the 'finiteness' of the fault surface – the fault ends, beyond the end of the mesh, are effectively locked, and so slip will tend to zero in those locations.

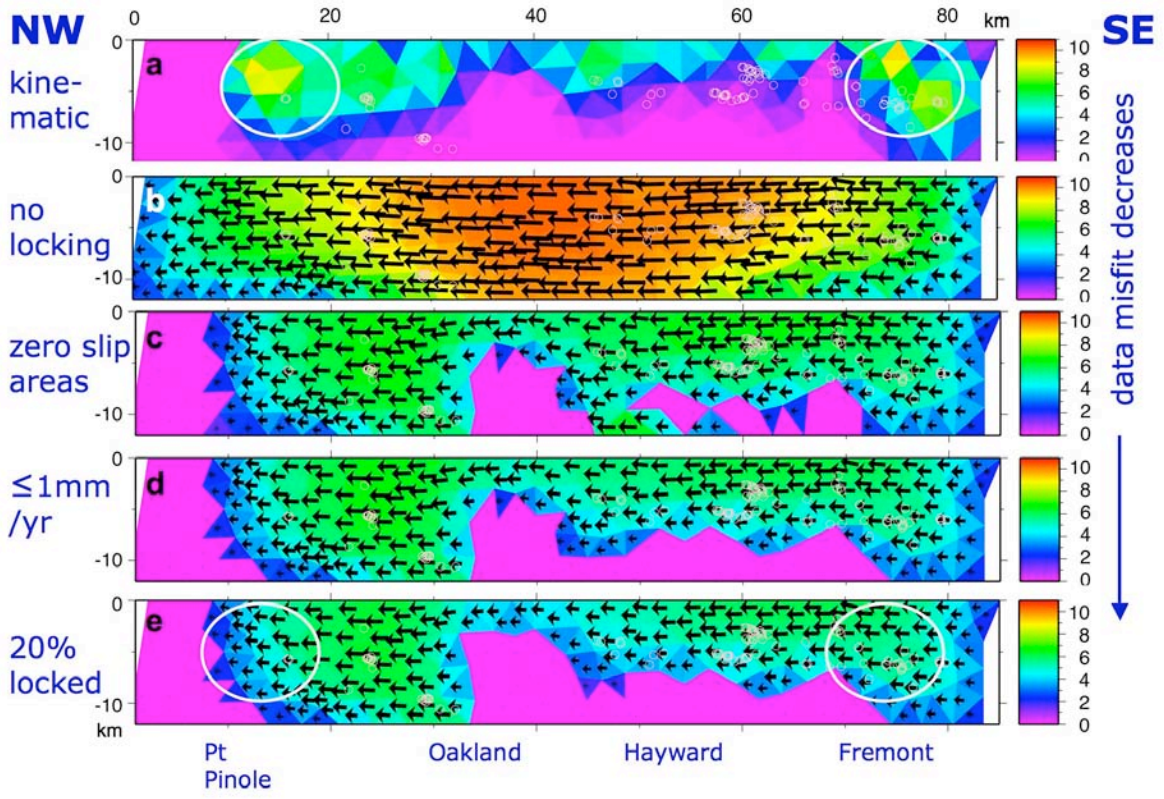

Figure 6: Models of creep and locking on the Hayward fault: *(a)* Kinematic inverse model. Pure right lateral slip is assumed. *(b)* Forward boundary element model (BEM) where no fault patches are assumed locked. *(c)* BEM where areas of zero slip in *(a)* are assumed to be locked. *(d)* BEM where areas of ≤1 mm/yr are assumed to be locked. *(e)* BEM with locked areas adjusted to prevent locking in areas of characteristic repeating earthquakes (small white circles), and to better fit surface creep rates. Large white circles indicate areas of elevated creep in the kinematic model that are not reproduced in the BEM.

Using this setup, we test a few scenarios based upon the kinematic model we obtained above (Figure 6). By locking all of the fault elements that showed zero slip in the kinematic model, we obtained the pattern shown in Figure 6c. This differs from the kinematic model significantly – creep rates are, on average, higher, and considerably more homogeneous in space. As may be expected, the data fit is substantially worse than that obtained in the kinematic modelling. The fit to data improved if data with creep rates of 1 mm/yr or lower were locked (Figure 6d), although the creep distribution was still too smooth to explain many of the observed features. A final iteration can be made by requiring creep in fault elements where characteristic repeating earthquakes (e.g. Schmidt et al., 2005), which are thought to be diagnostic of creep at those locations, occur. If this is applied as a constraint, and certain shallow patches are locked to better match surface creep rates in Oakland (Figure 6e) we arrive at our preferred boundary element model of the faulting. This shows the best data fit of the BEM based models.

The locked patch at the base of the fault which is picked out by this modeling covers approximately 20% of the surface of the fault (excluding the areas affected by the ends of the fault). This is consistent in broad terms with the rupture dimensions of the 1868 Hayward earthquake as estimated from triangulation data (Yu and Segall, 1996), and also with the distribution of damage from the earthquake (J Boatwright, personal communication). It is therefore reasonable to infer that this locked area is capable of supporting a future 1868-like earthquake. If we assume that the deep dislocation rate we obtained by kinematic modelling of 9.5 mm/yr is representative of the rate of motion of the Hayward fault over the whole of the current earthquake cycle, this locked patch would have accumulated a moment deficit equivalent to a Mw ~6.5 earthquake since 1868.

3.1.3. Questions Arising

The ultimate size of an earthquake that ruptured this asperity, however, would depend on the response of the creeping patches that surround the rupture. Most patches are slipping in the model at rates ~50% of the inferred long-term rate, and thus are storing elastic strain themselves. The question remains, would this stored moment be released in an earthquake, or afterwards as aseismic afterslip? The creeping elements of the Hayward fault are not creeping at the full loading rate, and so will be accumulating a moment deficit. The size of any future earthquake on the Hayward fault, or any of the other creeping faults, will depend on how this additional stored moment is released in the event of an earthquake – as coseismic or postseismic slip. In 2008, we submitted a proposal in collaboration with Kaj Johnson at Indiana University to tackle this problem by considering response of the Hayward fault to recent small earthquakes along the Hayward fault and rate-state frictional modeling of the aseismic creep behavior.

A suitable contemporary example would be the 2004 Parkfield earthquake, located at the southern end of the creeping central San Andreas fault, where it transitions into fully locked behavior. Surface slip occurred both coseismically and postseismically (Johanson et al., 2006); detailed modeling of coseismic and postseismic interferograms and local GPS observations suggests that only ~25% of the total moment release recorded occurred coseismically, with the areas of coseismic and postseismic slip spatially separated in the most part (Johanson et al., 2006). Analysis of triangulation network data of the Parkfield area, since reoccupied with GPS, shows that the coseismic slip patch is largely confined to the area which did not creep interseismically prior to the earthquake, which occurred in approximately the same location as the previous earthquake at Parkfield in 1966 (Murray and Langbein, 2006). The suggestion here is that the velocity-strengthening fault patches which enabled creep to occur before the earthquake, retained those properties during the coseismic disturbance and did not rupture, responding instead by creeping at an elevated rate in the days to weeks following the earthquake. Given the similarity in interseismic deformation behavior between the two faults, it should be a priority to understand and model such behavior so that the threat of any future earthquake on the Hayward fault is better understood.

There are significant differences between the two models generated of the Hayward fault creep (Figures 6a & 6e). The kinematic model is more heterogeneous, showing elevated creep rates in two areas in particular – at the NW end of the fault, near El Cerrito, and at the SE end of the fault at Fremont – which are larger than allowed by the instantaneous boundary element model. The latter creep feature represents a phenomenon that has been known for some time – that the creep rate at Fremont, measured by creepmeters to be ~8 mm/yr (Bilham and Whitehead, 1997), is significantly faster than that observed elsewhere on the Hayward fault, typically 3-5 mm/yr measured by alignment array (Lienkaemper et al., 2001). There are two possibilities as to why this might be occurring. The elevated rates that we observe could be the result of a temporal variations in rate due to frictional effects, e.g. creep oscillates between low rates (when friction is higher and additional strain is accumulated) and high rates (when friction is lower and this stored strain is released) on a ~decadal scale. Alternatively, an unmodeled near field source of deformation (Evans et al., 2007; Simpson et al., 2001), for instance a structural linkage to the Calaveras fault, could be supplying extra slip to the fault at that location.

There are observations to support both hypotheses. Fremont was the site of a creep event (aseismic slip at elevated rates) in 1996, where the fault moved 4.5 mm aseismically within 10 minutes (Bilham and Whitehead, 1997). 2 cm offsets at alignment arrays were also observed at this time (Galehouse and Lienkaemper, 2003). Thus it is likely that time-varying friction has some part to play in the behavior of the fault, at least at Fremont. We recently explored this

response in more detail employing a spring-slider representation of the creep response (Schmidt and Bürgmann, 2008) and found that the Hayward fault is likely to very sensitively respond to applied stress changes. Ingerestingly, this includes a likely reversal in fault creep to left-lateral slip in the aftermath of the 1906 San Andreas fault earthquake (Schmidt and Bürgmann, 2008). Structural linkages between the Calaveras and Hayward faults, on the other hand, have been suggested on the basis of GPS velocities, a band of microearthquakes that appear to link the two structures, and from the drop in surface creep rates on the Calaveras fault, north of the proposed junction (Andrews et al., 1993; Evans et al., 2007; Manaker et al., 2003; Manaker et al., 2005). We explore this question further in section 3.2, below.

3.2 Hayward – Calaveras Connection

Seismic studies of the Hayward-Calaveras step-over have suggested that the southern Hayward fault may dip into and merge with the central Calaveras Fault south of Fremont (Graymer et al., 2005; Manaker et al., 2005). This suggests that the Calaveras fault directly transfers slip to the Hayward Fault via a continuous structure. We find characteristic repeating earthquakes between 4 and 7 km depth in this region that indicate that active creep indeed occurs between the two faults.

Improved GPS-derived surface velocities and consideration of new PS-InSAR range-change rates in the Hayward-Calaveras stepover area help verify and constrain this proposed geometry, and allows a reevaluation of slip on these faults (Evans et al., 2007). A dislocation model combining seismically derived geometry and GPS velocities confirms that active fault creep occurs on the continuation of the dipping surface of the Hayward Fault effectively linking the Hayward and Calaveras Faults along a contiguous structure (Figures 7 and 8). The revised model provides an estimate of the distribution of creep on the three-dimensional fault surface through the stepover region, thus aiding in evaluating the seismic potential and rupture scenarios in the area.

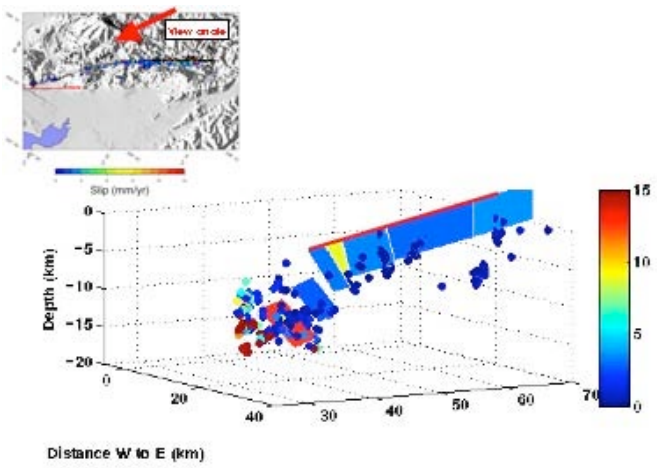

Figure 7: View from southeast looking at Hayward fault segments as used in the dislocation model. Hayward surface trace shown in red. The northernmost segments in the figure are vertical; progressing to the south, the patches dip as shallowly as 45°. Dots indicate location and slip rates of repeating microearthquakes, scaled with the same color scale (mm/yr). We find creep rates of 4mm/yr in the vertical segments (near Berkeley) with rates generally increasing towards the Calaveras. From Evans et al. (2007).

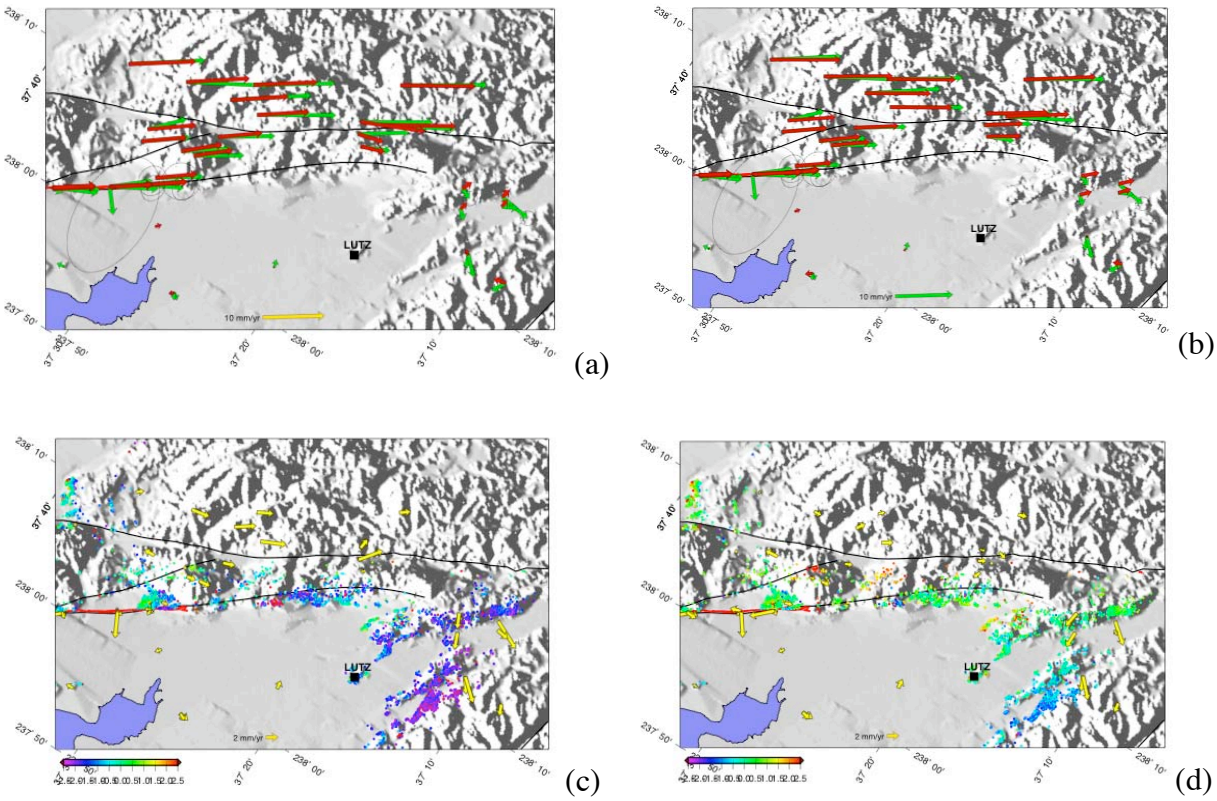

Figure 8: Comparison of modeled velocities and PS range change from (a), (c) a vertical Hayward fault model (from *Bürgmann et al*., 2006) and (b), (d) our dipping contiguous Hayward model (Figure 1). In general, the dipping Hayward causes residuals to greatly improve in the stepover region. From Evans et al. (2007).

3.3 Rodgers Creek Fault Creep

The GPS and PS-InSAR dataset covering the North Bay Area allows us to extend our analysis to the faults in that area. Deformation in the northern San Francisco Bay Area is dominated by a series of sub-parallel strike-slip faults. Existing GPS observations provide some constraint on the slip rates of these faults, however these have only limited resolution for resolving shallow fault behavior, such as brittle creep. The Rodgers Creek fault zone is seismically active and considered to pose a risk to nearby cities – in particular Santa Rosa, the largest city in the North Bay, which straddles the mapped fault trace (Figure 9). Two damaging (ML 5.6 and 5.7) earthquakes occurred on the fault just north of Santa Rosa in 1969, and paleoseismic investigations on its southern portion imply that the fault slipped 2 m in the last major ($M \approx 7$) event on that segment, probably in the 18th Century. Both the Hayward and Maacama faults, which link to the Rodgers Creek fault at its northwestern and southeastern extents, respectively, are known to undergo brittle creep in their upper portions, and it has been an open question whether the Rodgers Creek fault is behaving similarly.

Together with BAVU GPS data, we use the 30-image Permanent Scatterer InSAR dataset from ERS track 342 (Table 1) spanning the time interval 1992–2001 to dramatically increase the density of surface deformation observations. We find a discontinuity in observed surface velocities across the northernmost portion of the Rodgers Creek fault, around Santa Rosa and further north, which is consistent with shallow creep at rates of up to 6 mm/yr (Figure 9, Funning et al., 2007). We find that the Rodgers Creek fault is creeping at the surface with a rate of 4 ± 1 mm/yr at Santa Rosa. Creep may extend further to the NW, however there are insufficient points to make a determination of the rate. The creeping segments are located in areas of local transtension, suggesting that lowered normal stresses may play a role in the distribution of creep.The creeping segments are located in areas of local transtension, suggesting that lowered normal stresses may play a role.

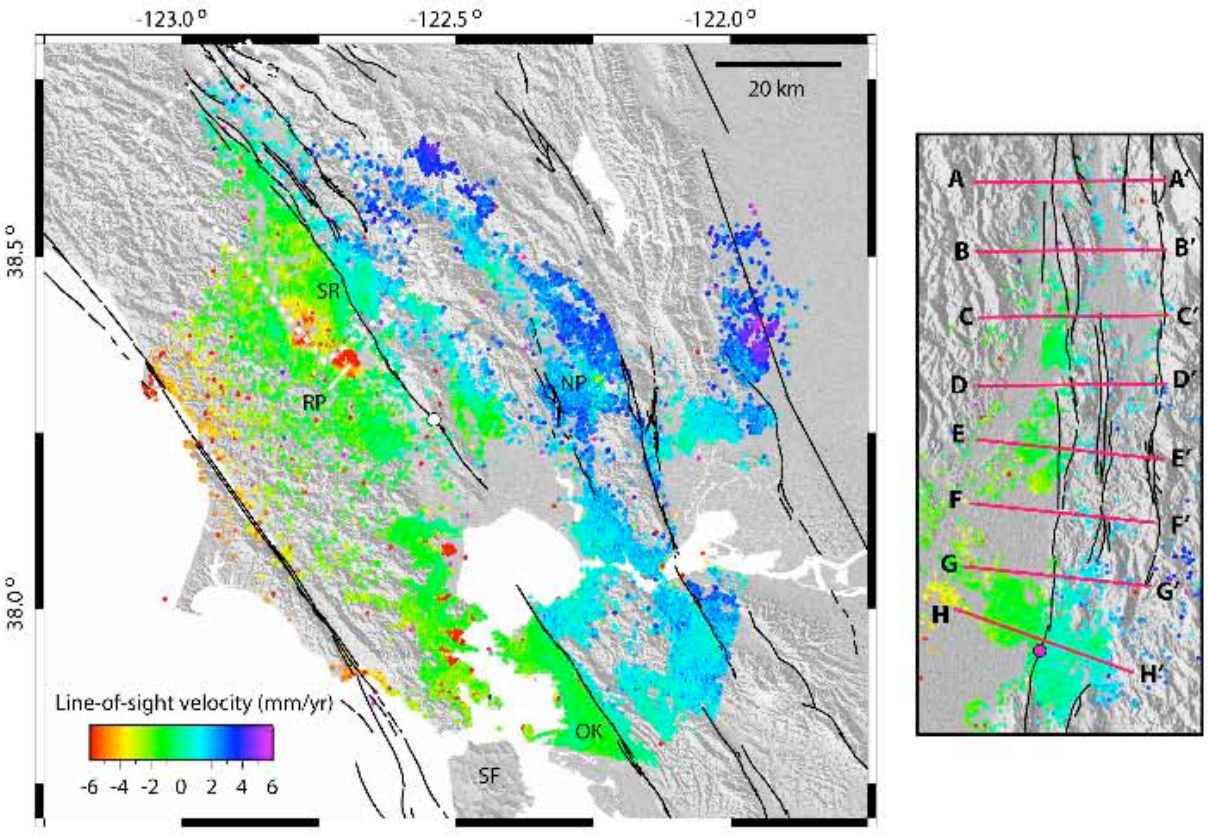

Figure 9: PS-InSAR data for the northern San Francisco Bay Area (track 342, frame 2835). Red colors indicate motion away from the satellite (range increase); blue, motion towards. SR: Santa Rosa, RP: Rohnert Park, NP: Napa, SF: San Francisco, OK: Oakland. Inset: Detail of velocities in the Santa Rosa area, after removal of points on weak substrate and thick sediment. From Funning et al. (2007).

Shallow brittle creep on other faults, in the San Francisco Bay Area and further south, is often accompanied by sequences of characteristic repeating earthquakes. The magnitudes and repeat intervals of these events can be related to the creep rate (e.g., Schmidt et al., 2005). Although, to our knowledge, no such earthquake sequences have been identified along the Rodgers Creek fault, the area has not hitherto been a target for such studies. Certainly, the distribution of earthquakes along the fault suggests some link between creep and microseismicity – cataloged seismicity shows that events are concentrated on the portion of the Rodgers Creek fault that we believe to be creeping, whereas the southern, locked, portion is largely aseismic.

Unlike along the central San Andreas fault, where recent evidence on the presence of talc, the weakest known natural mineral, at the location of the active creeping trace suggests that a mineralogical cause for the creep is plausible, it is difficult to infer such a cause for creep on the Rodgers Creek fault. The Santa Rosa segment of the Rodgers Creek fault where we observe creep (Figure 3) is surrounded at the surface by Plio-Pleistocene volcanics and Pleistocene

alluvial fan sediments, and geophysical data do not indicate the presence of large ultramafic bodies in the subsurface as seen on the San Andreas fault. Further to the southeast, the 40 km segment of fault that extends to San Pablo Bay is apparently locked. What, then, is the cause of this change in fault behavior at Santa Rosa? One clue may come from fault geometry. Santa Rosa itself lies within a releasing (right) bend on the Rodgers Creek fault, and is close to the mapped location of a releasing stepover to the Maacama fault. Each of these features would have a transtensional effect on the Santa Rosa area, reducing normal stress on the fault and therefore reducing frictional stresses, although model tests will be necessary to quantify the significance of the effect.

4. SIGNIFICANCE OF FINDINGS

The geodetic measurements help constrain the seismic potential of Bay Area faults, which can be used to further refine earthquake forecast probabilities. Detailed mapping of the locked asperity(ies) along the Hayward fault will help inform dynamic rupture scenarios and ground motion simulations of major earthquakes along the Hayward fault (Aagaard et al., 2008 Fall AGU). The contiguity of faulting and aseismic creep across the stepover region between the Hayward and Calaveras fault has important implications for rupture scenarios and mechanics of interaction between the two fault zones. We are currently exploring the implications of this finding, also in the context of the recent Alum Rock earthquake and its afterslip, which occurred at the southern end of the transfer structure. The existence of creep on the Rodgers Creek fault could reduce expected moment release in future earthquakes and will allow us to more precisely determine the rupture area of past and future large earthquakes on the fault, which thus has implications for seismic hazard assessment.

5. DATA AVAILABILITY

InSAR data collected by the ERS spacecraft used in this project have been obtained from the European Space Agency (ESA) and RADARSAT-1 data from the Alaska SAR facility (ASF). Much of these can be obtained via the WINSAR archive at UNAVCO. Inquiries for PS velocities and time series for research purposes can be made to Roland Bürgmann.

Data from GPS campaigns are publicly available from the UNAVCO Campaign Data Holdings Archive. Both raw GPS data and accompanying metadata are included and freely accessible at http://facility.unavco.org/data/gnss/campaign.php

Data collected by our group for this project are archived under the PI Name (Burgmann) for campaigns named "Calaveras Fault", "Hayward Fault", "Central San Andreas" and "Loma Prieta."

Please see http://www.unavco.ucar.edu/data_support/data/general.html for policies regarding the use of these freely available data. Additional data used in this study included RINEX format files obtained from the U.S. Geological Survey and the Bay Area Regional Deformation Network (BARD). These files include campaign-style surveying (USGS) and continuous GPS stations (BARD) and are available at the NCEDC at UC Berkeley.

Processed GPS solutions, including the BAVU velocity field, time series and GAMIT-format solution files (h-files) are available via the BAVU web pages at:

http://seismo.berkeley.edu/~burgmann/RESEARCH/BAVU/

http://seismo.berkeley.edu/~dalessio/BAVU/FILES/gamit.html

For more information regarding data availability, contact:

Dr. Roland Bürgmann
Department of Earth and Planetary Science, University of California, Berkeley
307 McCone Hall, Berkeley, CA 994720-4767
e-mail:burgmann@seismo.berkeley.edu

URL:http://www.seismo.berkeley.edu/~burgmann

5. REFERENCES

Andrews, D.J., Oppenheimer, D.H., and Lienkaemper, J.J., 1993, The Mission link between the Hayward and Calaveras faults: J. Geophys. Res., v. 98, p. 12083-12095.

Bilham, R., and Whitehead, S., 1997, Subsurface creep on the Hayward fault, Fremont, California: Geophys. REs. Lett., v. 24, p. 1307-1310.

Bürgmann, R., Hilley, G., Ferretti, A., and Novali, F., 2006, Resolving vertical tectonics in the San Francisco Bay area from GPS and Permanent Scatterer InSAR analysis: Geology, v. 34, p. 221-224.

Bürgmann, R., Schmidt, D., Nadeau, R., d'Alessio, M., Fielding, E., Manaker, D., McEvilly, T., and Murray, M.H., 2000, Earthquake potential along the northern Hayward fault: Science, v. 289, p. 1178-1182.

Cluff, B., and Steinbrugge, K.V., 1966, Hayward fault slippage in the Irvington-Niles Districts of Fremont, California: Bull. Seismol. Soc. Am., v. 56.

d'Alessio, M.A., Johansen, I.A., Bürgmann, R., Schmidt, D.A., and Murray, M.H., 2005, Slicing up the San Francisco Bay Area: Block kinematics and fault slip rates from GPS-derived surface velocities: J. Geophys. Res., v. 110, p. doi:10.1029/2004JB003496.

Evans, E., Bürgmann, R., and Nadeau, R.M., 2007, Linking Faults: Subsurface Creep on a Contiguous Fault Structure Connecting the Hayward and Calaveras Faults: Eos Trans. AGU, v. 88, p. Fall Meet. Suppl. Abstract S21A-0240.

Ferretti, A., Novali, F., Bürgmann, R., Hilley, G., and Prati, C., 2004, InSAR Permanent Scatterer Analysis Reveals Ups and Downs in the San Francisco Bay Area: Eos, v. 85, p. 317, 324.

Ferretti, A., Prati, C., and Rocca, F., 2001, Permanent scatterers in SAR interferometry: IEEE Trans. Geosci. Remote Sens., v. 39, p. 8-20.

Funning, G., Bürgmann, R., Ferretti, A., Novali, F., and Fumagalli, A., 2007, Creep on the Rodgers Creek fault from PS-InSAR measurements: Geophys. Res. Lett., v. 34, p. doi:10.1029/2007GL030836.

Galehouse, J.S., and Lienkaemper, J.J., 2003, Inferences drawn from two decades of alinement array measurements of creep on faults in the San Francisco Bay Region: Bull. Seism. Soc. Am., v. 93, p. 2415-2433.

Graymer, R.W., Ponce, D.A., Jachens, R.C., Simpson, R.W., Phelps, G.A., and Wentworth, C.M., 2005, Three-dimensional geologic map of the Hayward fault, northern California: Correlation of rock units with variations in seismicity, creep rate, and fault dip: Geology, v. 33, p. 521-524.

Hilley, G.E., Bürgmann, R., Ferretti, A., Novali, F., and Rocca, F., 2004, Dynamics of slow-moving landslides from permanent scatterer analysis: Science, v. 304, p. 1952-1955.

Johanson, I.A., Fielding, E.J., Rolandone, F., and Bürgmann, R., 2006, Coseismic and postseismic slip of the 2004 Parkfield earthquake from space-geodetic data: Bull. Seism. Soc. Am., v. 96, p. 269-282.

Lienkaemper, J.J., Galehouse, J.S., and Simpson, R.W., 2001, Long-term monitoring of creep rate along the Hayward fault and evidence for a lasting creep response to 1989 Loma Prieta earthquake: Geophys. Res. Lett., v. 28, p. 2265-2268.

Malservisi, R., Gans, C., and Furlong, K.P., 2003, Numerical modeling of creeping faults and implications for the Hayward fault, California: Tectonophysics, v. 361, p. 121-137.

Manaker, D.M., Bürgmann, R., Prescott, W.H., and Langbein, J., 2003, Distribution of interseismic slip rates and the potential for significant earthquakes on the Calaveras fault, central California: J. Geophys. Res., v. 108, p. doi:10.1029/2002JB001749.

Manaker, D.M., Michael, A.J., and Bürgmann, R., 2005, Subsurface structure and mechanics of the Calaveras Hayward fault stepover from three-dimensional vp and seismicity, San Francisco Bay region, California: Bull. Seism. Soc. Am., v. 95, p. 446-470.

Murray, J., and Langbein, J., 2006, Slip on the San Andreas Fault at Parkfield, California, over Two Earthquake Cycles, and the Implications for Seismic Hazard: Bull. Seis. Soc. Am., v. 96, p. S283 - S303.

Schmidt, D.A., and Bürgmann, R., 2003, Time dependent land uplift and subsidence in the Santa Clara valley, California, from a large InSAR data set: J. Geophys. Res., v. 108, p. doi:10.1029/2002JB002267.

—, 2008, Predicted reversal and recovery of surface creep on the Hayward fault following the 1906 San Francisco earthquake: Geophys. Res. Lett., v. 35, p. doi:10.1029/2008GL035270R.

Schmidt, D.A., Bürgmann, R., Nadeau, R.M., and d'Alessio, M.A., 2005, Distribution of aseismic slip-rate on the Hayward fault inferred from seismic and geodetic data: J. Geophys. Res., v. 110, p. doi:10.1029/2004JB003397.

Simpson, R.W., Lienkaemper, J.J., and Galehouse, J.S., 2001, Variations in creep rate along the Hayward fault, California, interpreted as changes in depth of creep: Geophys. Res. Lett., v. 28, p. 2269-2272.

Thomas, A.L., and Pollard, D.D., 1993, The geometry of echelon fractures in rock: Implications from laboratory and numerical experiments: J. Struct. Geol., v. 15, p. 323-334.

Yu, E., and Segall, P., 1996, Slip in the 1868 Hayward earthquake from the analysis of historical triangulation data: J. Geophys. Res., v. 101, p. 16101-16118.